

FIG. 9. (a) Longitudinal magnetoconductivity of sample 8B at  $1.3^\circ \text{K}$  as a function of magnetic field for several pressures. The straight portion of the dropoff is fitted to an expression derived from Kubo, Miyake, and Hashitsume (Ref. 35) (shown dashed). (b) Longitudinal magnetoconductivity of sample 7B1 at  $1.3^\circ \text{K}$ . Shubnikov-de Haas oscillations, which are not readily visible on this scale, are present in the dashed portion of the curves at low fields. (c) Longitudinal magnetoconductivity of sample 7B at  $4.2^\circ \text{K}$ .

more slowly with magnetic field than at helium temperatures.

Non-Ohmic behavior of sample 7B was observed at helium temperatures and at pressures up to 4 kbar. This could be seen on  $I$ - $V$  plots at various magnetic fields. But more features can be seen on the  $V$ - $B$  curves shown in Fig. 10, which is a photograph of the direct recorder traces of the voltage drop (or electric field) along the sample as a function of magnetic field at various constant currents. At currents below 1 mA the resistivity rises smoothly with magnetic field. At higher currents it rises more slowly and in particular shows a slight "knee" or discontinuity in slope. In Fig. 10 the positions of the knees are seen to fall on a straight line on the plot of electric field vs magnetic field. The top portion of Fig. 10 shows a plot of the derivative vs magnetic field of the 2-mA curve. In addition to the "knee" other structure with a complicated current dependence is observed. At 1 mA no corresponding structure (or knee) in the derivative could be detected. At present we do not understand this behavior.

#### ANALYSIS USING $k\vec{p}$ MODEL

The observed variation of the electron concentration with pressure  $P$  results from the pressure dependence of the energy gap  $E_g$ . We have fitted the  $n$ -vs- $P$  curve for sample 7B at 77 °K (Fig. 5) by assuming a linear pressure dependence:

$$E_g = E_0 + \alpha P,$$

where  $E_0$  is the energy gap at zero pressure,  $\alpha$  the pressure coefficient of  $E_g$ , and  $P$  the applied pressure. A similar method has been used by Schmit<sup>28</sup> to calculate the intrinsic concentration in  $\text{Hg}_{1-x}\text{Cd}_x\text{Te}$  alloys.

The concentration of ionized acceptors,  $N'_A$ , was assumed to be independent of pressure, and equal to  $1.5 \times 10^{16} \text{ cm}^{-3}$ , the value of  $p$  determined from the limiting value of  $R$  at high pressure. The position of the Fermi level was adjusted at each pressure until the calculated values of  $n$  and  $p$  satisfied the condition

$$p - n = N'_A.$$

The electron concentration was obtained by numerical integration of an expression given by Harman and Strauss<sup>29</sup> which is based on the Kane model and includes the effects of nonparabolicity and statistical degeneracy. A value of  $8.4 \times 10^{-8} \text{ eV cm}$  was used for the Kane matrix element. The valence band was assumed to be parabolic with an effective mass  $m_v^*$  and the hole concentration was obtained using the standard density-of-states expression. The calculations were made for masses between  $0.3m_0$  and  $0.7m_0$ , the range of values reported for  $m_v^*$  in  $\text{Hg}_{1-x}\text{Cd}_x\text{Te}$  and  $\text{HgTe}$ .<sup>5-11</sup>

The values of  $E_0$  and  $\alpha$  were adjusted to fit the calculated curve of  $n$  vs  $P$  to the experimental curve. The curve obtained for the two extreme values of  $m_v^*$  are shown in Fig. 5. The pressure coefficient in both cases is  $7.0 \times 10^{-3} \text{ eV/kbar}$  and the values for  $E_0$  are +2 and -8 meV for  $m_v^*$  of  $0.7m_0$  and  $0.3m_0$ , respectively. These may be compared with values of +11.6 and -15 meV obtained for  $x=0.15$  from empirical expressions for  $E_g(x, T)$  given by Wiley and Dexter<sup>8</sup> and Scott,<sup>30</sup> respectively. The behavior of the electron mobility shown in Fig. 6 is consistent with  $E_g=0$  near  $P=0$ . The failure to fit the experimental  $n$ -vs- $P$  data well at low pressures may be due to an incorrect choice of  $m_v^*$  or to the invalidity of the assumption that  $N'_A$  is constant. The latter will be strictly true only if the acceptor ionization energy is small relative to  $kT$ , and the analysis below indicates that the acceptor energy in this sample is comparable with  $kT$  at 77 °K. At higher pressure where  $N'_A \gg n$ , the slope in Fig. 5 is sensitive to the pressure coefficient, and relatively insensitive to the other parameters. The fitting at 77 °K should therefore yield a reliable value for  $\alpha$ .

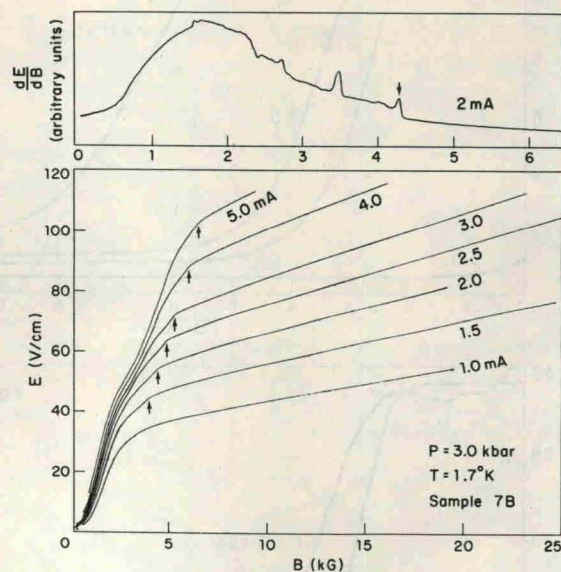


FIG. 10. Photograph of the direct recorder traces of the voltage drop (or electric field) along sample 7B as a function of magnetic field for several currents. (The sample cross-sectional area is  $2.5 \times 10^{-3} \text{ cm}^2$ .) The sample is non-Ohmic, since for  $B > 5 \text{ kG}$ ,  $E$  is not proportional to the current. In addition, structure is observed in the region  $1.5 < B < 6 \text{ kG}$  for sample currents greater than 1 mA. This structure is shown on an expanded scale by the derivative curve in the upper part of the figure. "Knees" appear in the curves at fields (4.25 kG on the 2-mA curve) which mark a disappearance of the structure. These "knees" marked by arrows are seen to fall on a straight line on the  $E$ -vs- $B$  plot.